

Cyprian Tyszko, Jacek Górka

# The Effect of the TIG Method-based Melting of Welds on the Properties and the Structure of Welded Joints Made of Austenitic Steel

---

**Abstract:** The article discusses the effect of TIG method-based melting on the properties and the structure of welded joints made of austenitic steel AISI 304. The tests involved the making of 2 mm thick joints followed by their subsequent melting performed in two different ways, i.e. with maintaining interpass temperature and immediately after welding. The study also included the performance of mechanical tests, macro and microscopic metallographic tests as well as hardness measurements and corrosion resistance tests. Results obtained in the tests justified the conclusion that the melting process and its conditions significantly affect the properties and the structure of welded joints.

**Keywords:** TIG welding, austenitic stainless steel, melting, interpass temperature, heat input

**DOI:** [10.17729/ebis.2022.1/4](https://doi.org/10.17729/ebis.2022.1/4)

---

## Introduction

Owing to their mechanical and physical properties, structural materials characterised by high corrosion resistance are used in many industrial sectors, including the petrochemical, food and automotive industries as well as, due to their aesthetics, in building engineering and architecture. Some of the most popular structural materials characterised by corrosion resistance are stainless steels. According to a report by the Grand View Research [1], in 2019 the international market of stainless steel was valued at 111.4 billion USD. Forecasts for 2027 estimate the growth of the aforesaid value up to 182.1 billion USD. The expected increase in the market value implies an increase in demand for stainless steel products both in

the heavy industry and as regards the production consumer goods. According to the same report, in 2019 steels of the 300 series (in accordance with the AISI/SAE standard) constituted 47.9% of the entire stainless steel market. Because of this, it can be assumed that stainless steels are and will remain the most commonly used stainless steels [1]. The making of a proper joint in austenitic steel requires not only significant knowledge but also complying with key principles before, during and after welding. As regards austenitic steels, each departure from technology could lead to the formation of welding imperfections or even the loss of corrosion resistance. In smaller businesses, which do not make structures based on the PN-EN 1090-2 standard [2], frequent reasons for the

---

mgr inż. Cyprian Tyszko – Silesian University of Technology; dr hab. inż. Jacek Górka, Professor at Silesian University of Technology

formation of imperfections are the fact that welded joints are made by low-skilled or unlicensed personnel or that welders deliberately ignore technological guidelines, which combined with the lack of inspections and acceptance of finished products leaves welders with leeway in terms of their “modifications” to the welding process. The above-presented factors and the susceptibility of steel X5CrNi18-10 to form intermetallic phase  $\sigma$ , high susceptibility to hot cracking and the precipitation of Nb, Cr and Ti carbides are responsible for the situation where each additional heat input (e.g. during melting aimed to eliminate weld asymmetry or the lack of penetration) can affect both the properties and the structure of joints. In terms of crucial structures, made in accordance with the requirements of standard [2], a given welding procedure must be qualified and the entire welding process must be supervised. However, as regards products which, in accordance with related regulations, do not require official certification or acceptance, there is a risk that, as a result of melting, the purchaser will receive an imperfect or even a defective product [1–7].

### Individual research

The research work aimed to identify the effect of TIG welding on the structure of welded joints made of austenitic steel X5CrNi18-10 (1.4301, 304). To this end, it was necessary to make 2 mm thick butt welded joints and, afterwards, to remelt two of them on the weld face side using various methods (with maintaining interpass temperature and without maintain the afore-said temperature, i.e. directly after welding). The chemical composition and the mechanical properties of the test steel are presented in Tables 1 and 2, whereas the structure of the steel is presented in Figure 1.

Table 2. Mechanical properties of 2 mm thick cold-rolled steel X5CrNi18-10 in accordance with PN-EN 10088-2 [8]

$R_{0,2}$ [N/mm <sup>2</sup> ]	$R_m$ [N/mm <sup>2</sup> ]	A [%]
≥ 230	540-750	≥ 45

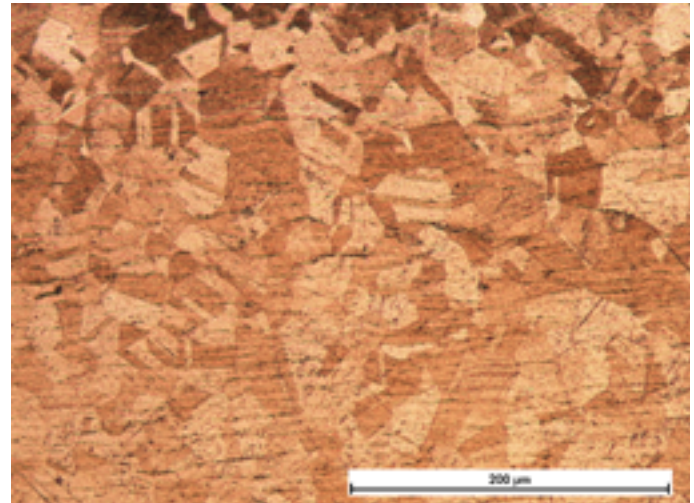


Fig 1. Microstructure of steel X5CrNi18-10; electrolytic etching in the solution of HNO<sub>3</sub> – distilled water

### Test joints

The joints used in the tests were made using the TIG (141) method and a Castolin Eutectic CastoTIG 2002 AC/DC welding machine and WT20 thoriated electrodes having a diameter of 2.4 mm (used in the DC reversed polarity welding of high-alloy steels). Before welding, the edges of the elements to be joined were subjected to milling, aimed to level the surface and remove areas thermally modified during cutting. Afterwards, to remove leftover grease, oil and steam, the edges and the adjacent area were cleaned using acetone. Because of the necessity of protecting the weld root when welding austenitic steels, the joints were made on a copper backing strip provided with ducts for backing gas. One of the sheets was fixed to the welding table using clamps. To prevent the movement of the elements in relation to one another it was necessary to make tack welds each 125 mm. The type of bevelling and the gap between the

Table 1. Chemical composition of steel X5CrNi18-10 (% by weight) according to the supplier (bal. Fe)

C	Si	Mn	P	S	Cr	Ni
0.05	0.42	1.35	0.035	0.014	18.2	8.75

elements subjected to welding were identified on the basis of the PN-EN ISO 9692-1 standard [9], stating that 2 mm thick butt welds should be welded single-sidedly. In accordance with the recommendations contained in the above-named standard, the test joints were made as square butt weld with gap  $b = 2$  mm. The filler metal used in the tests was a Lincoln Electric LNT 304L solid wire (W 19 9 L in accordance with PN-EN ISO 14343 [10]) having a diameter of 2 mm. In turn, the shielding and forming gas was gas from group I<sub>1</sub> (in accordance with the PN-EN ISO 14175 [11] standard), i.e. pure argon 5.0 (Air Liquide), having the commercial name of ALPHAGAZ 1 Ar. To facilitate the identification of individual test joints, the latter were designated as presented in Table 3.

Both the making and the melting of the welded joints were performed using the same parameters. The only difference was that the making of the welds involved the use of a filler metal, whereas the melting only involved the material of the previously made joint. The parameters of both processes (welding and melting) are presented in Table 4.

**Metallographic tests**

The macro and microscopic metallographic tests were performed using the specimens

Table 3. Designation of welded joints

Welded joint designation	Remarks
I	Single-run welded joint made using the filler metal
II	Single-run welded joint made using the filler metal, melted using an interpass temperature of 150°C
III	Single-run welded joint made using the filler metal, melted without maintaining an interpass temperature of 150°C

previously subjected to electrolytic etching in the solution of HNO<sub>3</sub> (distilled water (6:4)). The macrostructure was observed using an Olympus SZX9 microscope (Fig. 2), whereas the microstructure was observed using a Nikon Eclipse MA100 light microscope (Fig. 3 and 4).

**Hardness tests**

The hardness of the test joints was measured using the Vickers HV0.5 hardness test and a Wilson Wolpert Micro-Vickers 401 MVD machine. The measurements were initiated at the intersection of both axes of the weld cross-section. Afterwards, 15 measurements in each direction along the horizontal cross-sectional axis were performed (every 0.2 mm). The comparison

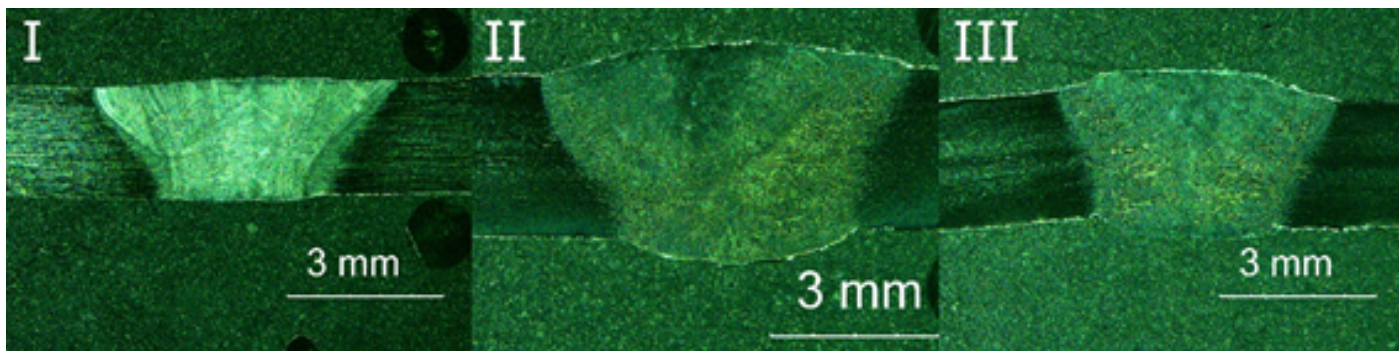


Fig. 2. Macrostructure of the test joints (joint designation at the top left-hand corner – in accordance with Table 3); electrolytic etching in the solution of HNO<sub>3</sub> – distilled water

Table 4. Parameters used during the welding and melting of test joints

Current I [A]	Voltage U [V]	Welding rate $V_{sp}$ [mm/s]	Shielding gas flow rate $Q_{ost.}$ [l/min]	Backing gas flow rate $Q_{form.}$ [l/min]	Welding current	Welding position	Gas nozzle number	Heat input Q [kJ/mm]
75	13	3	11	6	DC-	PA	6	0.234

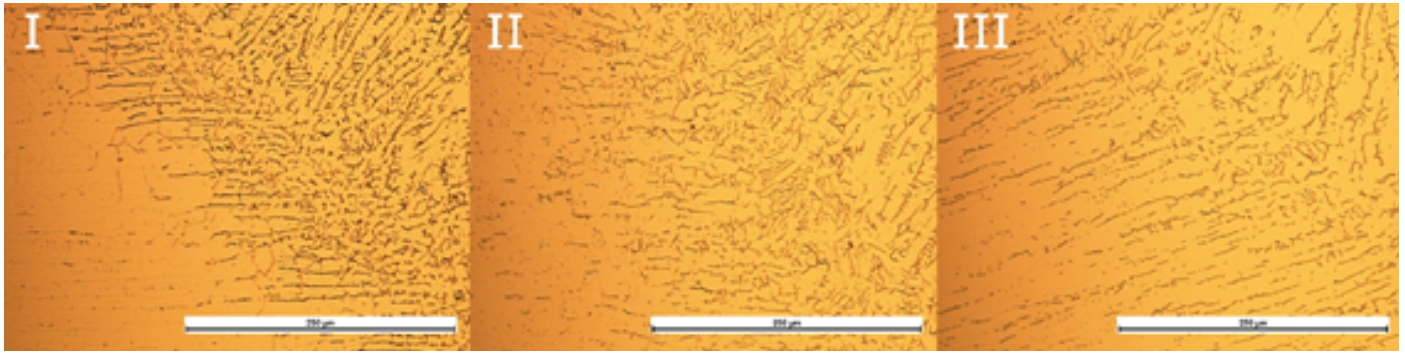


Fig. 3. Microstructure of the base material and of the HAZ in the test joints (joint designation at the top left-hand corner – in accordance with Table 3); electrolytic etching in the solution of HNO<sub>3</sub> – distilled water

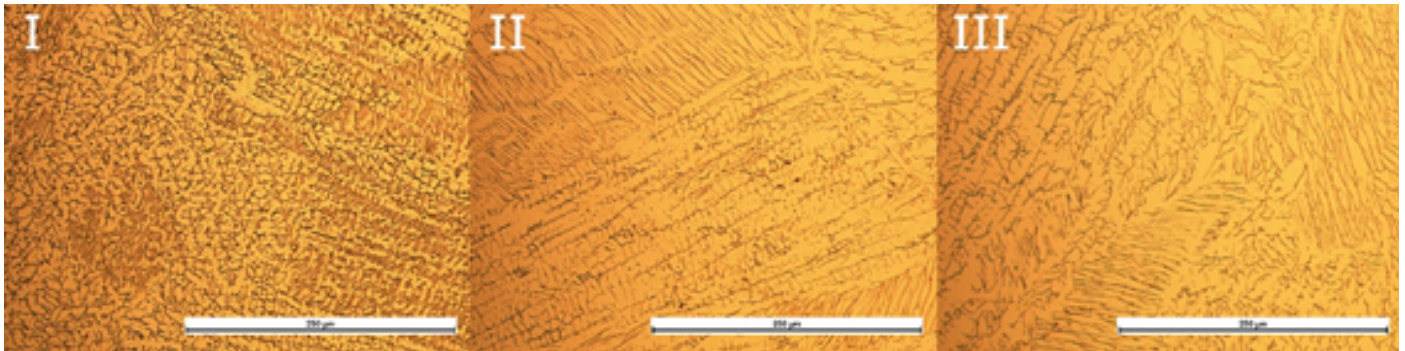


Fig. 4. Microstructure of the weld in the test joints (joint designation at the top left-hand corner – in accordance with Table 3); electrolytic etching in the solution of HNO<sub>3</sub> – distilled water

of the average hardness (HV<sub>0.5</sub>) of individual test joints (divided into zones) is presented in Figure 5.

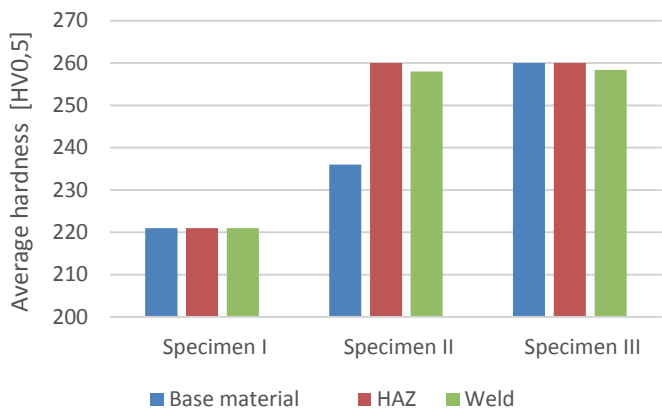


Fig. 5. Comparison of the average hardness (HV<sub>0.5</sub>) of the individual test joints (divided into zones)

### Strength tests

The face bend test (FBB) and the root bend test (RBB) of the butt weld were performed and their results were assessed in accordance with the PN-EN ISO 5173 standard [12]. The tests involved the use of a hydraulic press, a bending mandrel having a diameter of 12 mm and a bend angle of 135°. The static tensile test was

performed using a computer-controller testing machine provided with extensometers. The test was performed in accordance with the assumptions of the PN-EN ISO 6892-1 standard [13]. The results of the strength tests are presented in Table 5.

### Tests of corrosion resistance

The tests concerning general corrosion resistance in neutral salt spray (NSS) were performed in accordance with the requirements contained in the PN-EN ISO 9227 standard [14]. The test joints were placed in an Ascott CC450iP salt spray chamber and exposed to salt mist formed by mixing the 5% solution of NaCl with air having a temperature of 35°C. The time of exposure amounted to 168 hours. The test concerning resistance to intercrystalline corrosion in the environment of nitric acid (V) consisted in the immersion of the specimens in concentrated nitric acid (V), bringing the acid to boiling and maintaining the process for 48 hours. The results of the corrosion tests are presented in Table 6.

Table 5. Results obtained in the strength tests

Test joint	Tensile strength $R_m$ [MPa]	Elongation $A_t$ [%]	Bend angle [°]	Assessment result
I	626	52,5	135	positive
II	625	46	135	positive
III	628	47,5	135	positive

Table 6. Corrosion test results

Test joint	NSS		Huey test	
	Mass decrement $V_c$ [g/m <sup>2</sup> /24h]	Linear corrosion rate $V_g$ [mm/year]	Mass decrement $V_c$ [g/m <sup>2</sup> /24h]	Linear corrosion rate $V_g$ [mm/year]
I	0.01653	$7.63 \times 10^{-5}$	17.1519	0.0792
II	0.02874	$1.32 \times 10^{-4}$	3.8310	0.0177
III	0.03184	$1.47 \times 10^{-4}$	16.1322	0.0742

## Analysis of results

The macroscopic test results revealed that none of the test joints contained internal welding imperfections. Only in the unmelted joint it was possible to notice the clearly visible fusion line and the heat affected zone. The structure of each specimen was dendritic, which resulted from the non-uniform discharge of heat during solidification. The dendritic structure was particularly visible in the joint melted without maintaining the interpass temperature. The microscopic tests of the base material revealed the presence of recrystallisation twins and banded ferrite  $\delta$ , resulting from the cold rolling process and the segregation of ferrite-forming elements. In each test joint, the HAZ had the austenitic structure with precipitates of skeletal ferrite  $\delta$  and interdendritic ferrite. It was also possible to observe that the austenite grain size was the smallest in the HAZ of the joint not subjected to melting and the largest in the joint subjected to melting without maintaining interpass temperature. Both in the base material and in the HAZ of the joint not subjected to melting and in the joint subjected to melting with maintaining interpass temperature it was possible to observe precipitates of the  $Cr_{23}C_6$  chromium carbides and phase  $\sigma$  in the austenite–ferrite division areas. In turn, the aforesaid precipitates dissolved in the joint subjected to

melting without maintaining interpass temperature. In each of the test joints the weld structure was austenitic and contained precipitates of ferrite  $\delta$  in the skeletal or lath form. In the weld not subjected to melting, the areas of skeletal ferrite contained clearly visible precipitates of phase  $\sigma$ , whereas throughout the weld it was possible to observe uniformly arranged chromium carbides ( $Cr_{23}C_6$ ). The weld subjected to melting with maintaining interpass temperature contained traces of precipitates. In turn, similar to the HAZ and the base material, precipitates nearly entirely dissolved in the weld subjected to melting performed directly after welding. The decrease in the amount of post-melt precipitates was accompanied by the significant growth of the austenite grain, particularly in the joint which was melted without maintaining interpass temperature. The Vickers HV<sub>0.5</sub> test revealed that the hardness of each zone of the test joint not subjected to melting was restricted within the range of values declared by major producers of steel X5CrNi18-10 (i.e. 226 HV). In cases of the joints subjected to melting, each of the zone underwent hardening. The growth of hardness was the highest in the joint subjected to melting without maintaining interpass temperature and was by approximately 30 HV<sub>0.5</sub> higher than the maximum values declared in relation to the test steel. The FBB and

RBB tests in relation to an angle of  $135^\circ$  did not reveal any damage to the joints. In the specimen not subjected to melting, bending took place in the weld area. In turn, in the specimens subjected to melting, bending took place outside the weld, thus confirming the hardening of the weld area in relation to the base material. The static tensile test revealed that the tensile strength of all the specimens was restricted within the range of 625 MPa to 628 MPa, which demonstrated the negligible effect of melting on the above-named parameter. Each specimen ruptured in the base material area. The melting process visibly worsened the elongation of the specimens, yet in relation to each of the joints, elongation values were restricted within the range specified in the PN-EN 10088-2 standard [8]. The NSS corrosion test results revealed that the linear corrosion rate was the highest in relation to the joint subjected to melting without maintaining interpass temperature and the lowest in terms of the joint not subjected to melting. The foregoing resulted from the more intense oxidation of the surfaces of the joints subjected to melting in comparison with that of the single-run welded joint. The Huey test results revealed that the joint subjected to melting with maintaining interpass temperature was characterised by the highest corrosion resistance, which could be ascribed to the lower content of carbides in comparison with that observed in the joint not subjected to melting as well as to the lower segregation of alloying elements in relation to noticed in the joint subjected to melting directly after welding.

## Conclusions

The tests concerning the effect of the TIG method-based melting of the weld on the properties and the structure of the welded joints made of austenitic steel led to the conclusions presented below.

1. A repeated heat input during the TIG method-based melting of the joints changed the structure, properties and the corrosion resistance of the joints.

2. The melting of the joint with maintaining interpass temperature dissolved most chromium carbides ( $\text{Cr}_{23}\text{C}_6$ ) and precipitates of phase  $\sigma$ , yet it also led to the austenite grain growth.

3. The melting of the joint without maintaining interpass temperature dissolved almost all chromium carbides ( $\text{Cr}_{23}\text{C}_6$ ) and the precipitates of phase  $\sigma$ , yet, the accompanying austenite grain growth was significantly higher than that observed in the specimen not subjected to melting or the specimen subjected to melting with maintaining interpass temperature.

4. The melting of the joint increased its hardness in comparison with that of the joint not subjected to melting. The aforesaid increase could result from the austenite grain growth.

5. The melting of the joint proved to have a negligible effect on both the bending strength and the tensile strength of the joints.

6. The melting of the joint decreased the relative elongation of the welded specimens in comparison with that of the specimens not subjected to melting.

7. Because of the more intense post-weld oxidation, the melting of the joint decreased its general corrosion resistance.

8. The melting of the joint increased its resistance to intercrystalline corrosion, which could be attributed to the dissolution of the precipitates of phase  $\sigma$  and of chromium carbides ( $\text{Cr}_{23}\text{C}_6$ ).

9. In comparison with the joint subjected to melting with maintaining interpass temperature, the joint subjected to melting without maintaining interpass temperature was characterised by higher hardness, lower resistance to general and intercrystalline corrosion and improved relative elongation.

In terms of the joints made of thin austenitic steel sheets, the melting process led to the deterioration of joint properties. On the other hand, because of the solution of the precipitates of phase  $\sigma$  and of chromium carbides, resistance to intercrystalline corrosion improved. However, the significant oxidation of the joint surface

combined with the austenite grain growth decreased the resistance of the joint to general corrosion, reduced the elongation of the joint and increased its hardness above maximum values declared by the manufacturers of the base material. The microstructural tests and hardness measurements also implied that the joint subjected to melting could be characterised by worse toughness, which, however, could not be verified because of the overly thin elements subjected to welding. To obtain joints characterised by the optimum combination of mechanical and plastic properties as well as of corrosion resistance, it is necessary to avoid the melting of joints.

## References

- [1] Grand View Research: Stainless Steel Market Size, Share & Trends Analysis Report By Grade (200 Series, 300 Series, 400 Series, Duplex Series), By Product (Flat, Long), By Application (Building & Construction, Heavy Industry), By Region, And Segment Forecasts. [online], access date: 13.06.2021, <https://www.grandviewresearch.com/industry-analysis/stainless-steel-market>.
- [2] PN-EN 1090-2:2019-09. Wykonanie konstrukcji stalowych i aluminiowych – Część 2: Wymagania techniczne dotyczące konstrukcji stalowych.
- [3] Di Schino A.: Manufacturing and Application of Stainless Steels. MPDI AG, Basel, 2020.
- [4] Tasak E., Ziewiec A.: Spawalność materiałów konstrukcyjnych. Tom 1. Spawalność Stali. Wydawnictwo JAK, Kraków 2009.
- [5] Łabanowski J.: Stale odporne na korozję i ich spawalność. Wydawnictwo Politechniki Gdańskiej, Gdańsk 2019.
- [6] Folkhard E.: Welding Metallurgy of Stainless Steels. Springer-Verlag, Wien 1984.
- [7] Lippold J., Kotecki D.: Welding metallurgy and weldability of stainless steels. John Wiley & Sons, Inc., New Jersey 2005.
- [8] PN-EN 10088-2:2014-12. Stale odporne na korozję – Część 2: Warunki techniczne dostawy blach cienkich/grubych i taśm ze stali nierdzewnych ogólnego przeznaczenia.
- [9] PN-EN ISO 9692-1:2014-02. Spawanie i procesy pokrewne – Rodzaje przygotowania złączy – Część 1: Ręczne spawanie łukowe, spawanie łukowe elektrodą metalową w osłonie gazów, spawanie gazowe, spawanie metodą TIG i spawanie wiązką stali.
- [10] PN-EN ISO 14343:2017-06. Materiały dodatkowe do spawania – Druty elektrodowe, taśmy elektrodowe, druty i pręty do spawania łukowego stali nierdzewnych i żaroodpornych – Klasyfikacja.
- [11] PN-EN ISO 14175:2009. Materiały dodatkowe do spawania – Gazy i mieszaniny gazów do spawania i procesów pokrewnych.
- [12] PN-EN ISO 5173:2010/A1:2012. Badania niszczące spoin w materiałach metalowych – Badanie na zginanie.
- [13] PN-EN ISO 6892-1:2020-05. Metale – Próba rozciągania – Część 1: Metoda badania w temperaturze pokojowej.
- [14] PN-EN ISO 9227:2017-06. Badania korozyjne w sztucznych atmosferach – Badania w rozpylonej solance.
- [15] Effect of TIG melting on properties and structure of welded joints of austenitic stainless steel